

# Catalytic Properties of Framework $\text{Fe}^{3+}$ in MFI-Type Ferrisilicate: Reaction Mechanism Studies of CO Oxidation Using an Isotopic Tracer Technique

Md. Azhar Uddin, Takayuki Komatsu, and Tatsuaki Yashima<sup>1</sup>

*Department of Chemistry, Tokyo Institute of Technology, 2-12-1 Ookayama, Meguro-ku, Tokyo 152, Japan*

Received July 1, 1993; revised November 3, 1993

The catalytic properties of  $\text{Fe}^{3+}$  in the framework sites of MFI-type ferrisilicate were studied by comparing with iron-oxide-impregnated silicalite ( $\text{FeO}_x/\text{Sil}$ ) for the oxidation of CO with  $\text{O}_2$ . On  $\text{FeO}_x/\text{Sil}$  the reaction proceeds via a redox mechanism where CO is oxidized with the lattice oxygen of the catalyst (iron oxide), while on ferrisilicate, the CO oxidation occurs by the reaction of CO with the oxygen from the gas phase. These mechanisms were confirmed by kinetic and isotopic tracer results. The CO oxidation with  $^{18}\text{O}_2$  on ferrisilicate revealed significant incorporation of lattice oxygen into product  $\text{CO}_2$  produced. The CO oxidation mechanism on ferrisilicate was explained as follows:  $\text{CO}_2$  is produced by reaction between CO and gas phase oxygen; heterophase exchange between lattice oxygen and  $\text{CO}_2$  occurs at a significant rate; furthermore, oxygen isotope equilibration in  $\text{CO}_2$  occurs simultaneously. On  $\text{FeO}_x/\text{Sil}$ , the amount of lattice oxygen incorporated into  $\text{CO}_2$  during CO oxidation with  $^{18}\text{O}_2$  was very small. The CO oxidation mechanism on  $\text{FeO}_x/\text{Sil}$  was explained as follows: lattice oxygen in the surface layer of  $\text{Fe}_2\text{O}_3$  crystallite in  $\text{FeO}_x/\text{Sil}$  oxidizes CO into  $\text{CO}_2$ , and the reduced surface site is rapidly reoxidized with gas phase oxygen. As the reaction proceeds, the surface lattice oxygen is almost replaced by gas phase oxygen because the scrambling of the lattice oxygen between the surface layer and the bulk of  $\text{Fe}_2\text{O}_3$  occurs much more slowly than CO oxidation. © 1994

Academic Press, Inc.

based on the metal or metal cation in a particular oxidation state are generated, or grafting a given compound onto the outer surface or into the inner pore of the zeolite crystallite by chemical reaction with external or internal OH groups. Incorporation of transition metal cations into zeolite by methods other than isomorphous substitution often alters the pore size of the zeolite (2), whereas isomorphous substitution of metal cations into the zeolite framework does not affect the pore size significantly. It is obvious that chemical and subsequently catalytic properties differ depending on the way the foreign element has been incorporated.

Substitution of various kinds of metal ions into the zeolite framework induces acidic and catalytic properties different from the usual aluminosilicate zeolites (3). Much of the research in the field of metallosilicate catalysis has been related to reactions where the zeolite is used as a solid acid, e.g., isomerization, cracking, hydrocracking (4-9). These studies have utilized the acid property of framework OH groups connected to the incorporated transition metal cation in metallosilicate rather than the activity of the incorporated metal cation itself. Some research on metallosilicates has indicated that the incorporated transition metal cation in the metallosilicate framework itself can be a catalytically active center. Notari has studied the synthesis and catalytic properties of MFI-type titanosilicate which possesses no acid sites (acidic OH group) and indicated that  $\text{Ti}^{4+}$  ions in titanosilicate are active in the hydroxylation, oxidation, and epoxidation of various kinds of hydrocarbons (10). Miyamoto *et al.* have studied the catalytic properties of MFI-type vanadosilicates for the oxidation of  $\text{H}_2$  and  $\text{NH}_3$  with  $\text{O}_2$ , reduction of NO with  $\text{NH}_3$ , and ammoxidation of xylenes (11). They have reported that the catalytic behavior of vanadosilicates differs markedly from that of conventional vanadium oxide (bulk  $\text{V}_2\text{O}_5$ ). However, very little attention has been paid to the catalytic properties of other transition metal ions located in metallosilicate framework sites.

## INTRODUCTION

With the growth of interest in using zeolites as catalysts, more attention has been paid to the isomorphous substitution of other elements for aluminum in the zeolite framework. The purpose of isomorphous substitution is to modify the chemical and physical properties of zeolites to obtain new catalytic properties while maintaining the original crystal structure. The physical and chemical properties of zeolites can be altered in other ways (1) such as by exchanging alkaline cations with other cations which exhibit different chemical properties as such or after reduction to form metallic particles, impregnating a given metal precursor onto a zeolite support so that active sites

<sup>1</sup> To whom correspondence should be addressed.

According to Lowenstein's rule (12), there is no Al–O–Al linkage in aluminosilicate (zeolite). In metasilicates, all metal cations, such as aluminum in zeolite, occupy tetrahedral coordination sites surrounded by SiO<sub>4</sub> tetrahedra and are, therefore, isolated from each other. In other words, the incorporation of transition elements into framework positions of metasilicates provides a novel means of obtaining high dispersions of these elements within the zeolite structure. However, in pure metal oxides, the metal cations are connected to each other by O<sup>2-</sup> and the metal ions are present in chemical states different from those in the metasilicates. Therefore, it is expected that metal cations of metasilicates occupying tetrahedral sites will show catalytic properties different from those of pure metal oxides.

It is generally known that the oxides of transition metals, both pure and mixed, are active catalysts for the oxidation of carbon monoxide with oxygen. The activity of, and reaction mechanism on, metal oxides varies greatly depending on the chemical states, such as oxidation and coordination states, of the metal cation in the oxide host matrix. Catalytic properties of several transition metal ion-exchanged zeolites for the oxidation of CO have been reported (13–21). Fe-Y, Fe-X and Fe-mordenite have been shown to act as catalysts for the oxidation of CO with O<sub>2</sub> (18–20). By studying the kinetics of CO oxidation with O<sub>2</sub> on iron-exchanged zeolites (Fe-Y, Fe-mordenite), Petunchi and Hall (20) concluded that the reaction proceeds via a redox mechanism. However, no such studies concerning the catalytic properties of the metal ions present in the tetrahedral framework sites of metasilicates have been carried out thus far.

Mössbauer spectroscopy has shown that the Fe ions in ferrisilicate are tetrahedrally coordinated Fe<sup>3+</sup> (22, 23) and that those in iron oxide supported on silicalite or silica are octahedrally coordinated Fe<sup>3+</sup> in the form of small particles of  $\alpha$ -Fe<sub>2</sub>O<sub>3</sub> (23, 24). We have reported (23) that the activity (per Fe atom) of tetrahedrally coordinated Fe<sup>3+</sup> in ferrisilicate framework for CO oxidation with O<sub>2</sub> was much lower than that of the octahedrally coordinated Fe<sup>3+</sup> in the iron-oxide-impregnated silicalite or that of Fe cations in FeZSM-5 prepared by an ion-exchange method. The partial pressure dependencies of the CO oxidation rate on ferrisilicate were different from those on the iron-oxide-impregnated silicalite and FeZSM-5. The purpose of this study is to elucidate the catalytic behavior of framework iron in MFI-type ferrisilicate for CO-oxidation in view of the mechanistic aspects of the oxidation reaction. For comparison, the same reaction was performed on iron-oxide-impregnated silicalite, which contains oxides of iron precipitated on MFI-type silicalite. In these catalysts, Fe<sup>3+</sup> ions are in the matrix or on the support with the same MFI structure. Through the use of tracer tech-

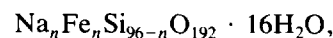
CO oxidation on ferrisilicate and iron-oxide-impregnated silicalite.

## EXPERIMENTAL

### *Synthesis and Characterization of Catalysts*

The synthesis of ferrisilicate with MFI structure was carried out hydrothermally (25, 26). The reaction gel was prepared by mixing appropriate quantities of sodium silicate solution (9.28 wt% Na<sub>2</sub>O, 28.93 wt% SiO<sub>2</sub>, and 61.79 wt% H<sub>2</sub>O), Fe(NO<sub>3</sub>)<sub>3</sub> · 9H<sub>2</sub>O, sulfuric acid (98%), tetra-*n*-propylammonium bromide (TPABr), and deionized water. The molar composition of the synthesis slurry was 31.2 Na<sub>2</sub>O, 100 SiO<sub>2</sub>, 1.0 Fe<sub>2</sub>O<sub>3</sub>, 2810 H<sub>2</sub>O, and 9.5 TPABr. Hydrothermal synthesis was carried out at 438 K for 3 days. The product was filtered, washed, and dried at 393 K overnight and then calcined at 773 K for 4 h in air. The synthesis of silicalite was carried out using the procedures outlined in references (27). Iron-oxide-impregnated silicalite (FeO<sub>x</sub>/Sil) was obtained by impregnating the silicalite with an aqueous solution of Fe(NO<sub>3</sub>)<sub>3</sub> in a conventional manner, followed by drying at 393 K overnight and calcining at 773 K for 4 h in air.

The unit-cell formula of MFI-type ferrisilicate is represented by



where *n* represents both the number of framework Fe ions and the number of charge compensating sodium cations.

The structural identification and crystallinity of the samples were checked by powder X-ray diffraction. Elemental analyses were performed by atomic absorption spectrophotometry. The Si/Fe atomic ratio for ferrisilicate was 47. The iron content in iron-oxide-impregnated silicalite (FeO<sub>x</sub>/Sil) was 1.9 wt% which corresponds to a Si/Fe atomic ratio of 50. The specific surface areas of ferrisilicate and silicalite are 430 and 530 m<sup>2</sup> g<sup>-1</sup>, respectively.

### *Isotopic Tracer Experiments*

Isotopic tracer experiments were carried out in a glass circulation system with a dead volume of 315 ml. CO (99.9%) was passed through a silica gel trap at acetone dry-ice temperature to remove water before introduction into the system. <sup>18</sup>O<sub>2</sub> and C<sup>18</sup>O<sub>2</sub> (99 at% <sup>18</sup>O) were used as supplied. The catalyst, placed in a reactor connected to the fixed-volume glass circulation system, was degassed in a vacuum at 773 K for 1 h. After the catalyst had been isolated from the vacuum line and cooled to reaction temperature, the catalytic reaction was commenced by circulating a reactant gas mixture. The reac-

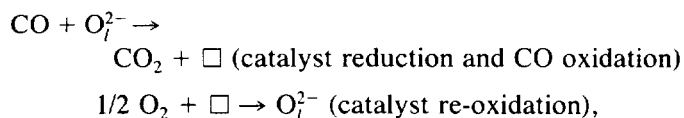
fraction of the gas mixture through a glass capillary leak into the ionization region of a quadrupole-mass spectrometer (Ulvac, MSQ-150A). The volume of the sampling portion was such that the quantity of gas in the system was reduced by less than 1% per sampling. The relative amount of oxygen isotopes ( $^{16}\text{O}$  and  $^{18}\text{O}$ ) in gaseous oxygen, carbon monoxide, and carbon dioxide were determined by mass spectrometry assuming the same ionization efficiency for the molecules containing  $^{16}\text{O}$  and/or  $^{18}\text{O}$ . Reaction conditions for each tracer experiment will be stated in the next section.

## RESULTS AND DISCUSSION

### Catalytic Tests and Kinetic Studies

The CO oxidation is first order with partial pressure of both CO and  $\text{O}_2$  for ferrisilicate; it is first order with CO and zero order with  $\text{O}_2$  for both  $\text{FeO}_x/\text{Sil}$  and  $\text{FeZSM-5}$  (23). Kinetic studies of CO oxidation with  $\text{O}_2$  on Fe-Y and Fe-mordenite gave results similar to the latter case, i.e., the first order with CO and the zero order with  $\text{O}_2$  (20, 21). Through the use of a TGA technique, it was concluded (20) that the reaction on Fe-Y and Fe-mordenite proceeds via a redox mechanism where the reduction of Fe ions in the catalyst is the rate limiting step.

From the kinetic results, we can tentatively suggest the reaction mechanism of CO oxidation on ferrisilicate and  $\text{FeO}_x/\text{Sil}$ . In the case of ferrisilicate, the CO oxidation with  $\text{O}_2$  follows a reaction mechanism in which CO is oxidized with oxygen of gas phase origin; that is, the lattice oxygen of ferrisilicate does not oxidize CO. In the case of  $\text{FeO}_x/\text{Sil}$ , however, the reaction proceeds through a redox mechanism where CO is oxidized with the lattice oxygen of the catalyst. The overall rate is limited by the reduction step of the catalyst. This can be described as



where  $\text{O}_i^{2-}$  represents a lattice oxygen of  $\text{Fe}_2\text{O}_3$  in  $\text{FeO}_x/\text{Sil}$ , and  $\square$  denotes an oxygen vacancy caused by the removal of an  $\text{O}_i^{2-}$  from the site. The major differences in the catalytic properties between ferrisilicate and  $\text{FeO}_x/\text{Sil}$  could be the reactivity of the lattice oxygen with CO.

### CO Oxidation without Gas Phase Oxygen

The purpose of this experiment was to clarify the reactivity of lattice oxygen for CO oxidation on ferrisilicate and  $\text{FeO}_x/\text{Sil}$  in the absence of gas phase oxygen. The reaction was carried out under the following conditions: initial pressure of CO, 10 Torr; reaction temperature, 673 K; amount of catalyst, 0.10 g. Figure 1 shows CO

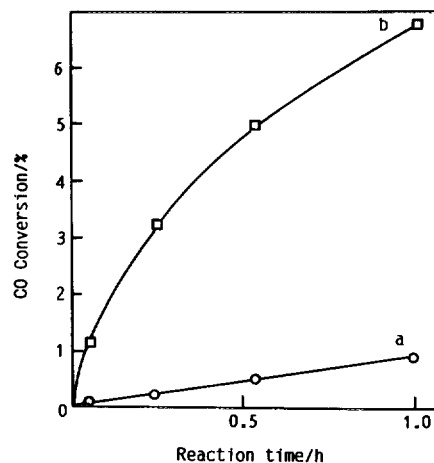


FIG. 1. CO oxidation without gas phase oxygen at 673 K on (a) ferrisilicate and (b)  $\text{FeO}_x/\text{Sil}$ . Weight of catalyst was 0.10 g in both cases. Initial pressure of CO was 10 Torr.

conversion on ferrisilicate and  $\text{FeO}_x/\text{Sil}$  for CO oxidation performed at 673 K without gas phase oxygen. On ferrisilicate (a), the reaction proceeded very slowly: a conversion of less than 1% was achieved after 1 h of reaction time, while on  $\text{FeO}_x/\text{Sil}$  (b) CO conversion reached 6.7%. In both cases, the deposition of carbon, which may be due to CO disproportionation, was observed on the used catalyst. Some contribution of CO disproportionation to the overall CO conversion cannot be ruled out from these results. Under similar reaction conditions but in the presence of gas phase oxygen, after 1 h of reaction time the conversions of CO oxidation on ferrisilicate and  $\text{FeO}_x/\text{Sil}$  were 13% and 79%, respectively (19). It is clear that without gas phase oxygen the rate of CO oxidation on ferrisilicate is very slow compared with CO oxidation in the presence of gas phase  $\text{O}_2$ .

### Isotopic Tracer Studies

CO oxidation was further studied using an isotopic tracer technique to confirm and improve the mechanism postulated from the above kinetic results.

### CO Oxidation with $^{18}\text{O}_2$ on Ferrisilicate

The kinetic studies suggested that CO oxidation on ferrisilicate occurs via a surface reaction of adsorbed CO with adsorbed oxygen and that the lattice oxygen of ferrisilicate may have no direct role in the CO oxidation mechanism. An attempt was made to examine the role of lattice oxygen in the CO oxidation on ferrisilicate using  $^{18}\text{O}_2$  as a tracer. The reaction was carried out under the following conditions: initial pressure,  $P(\text{CO}) = P(^{18}\text{O}_2)$ , 20 Torr; amount of catalyst, 25 mg; reaction temperature, 673 K. The reaction was followed by analyzing the reaction mixture with a quadrupole mass spectrometer at various reac-

tion times. The CO conversion and the mole fractions of  $\text{CO}_2$  produced ( $\text{C}^{16}\text{O}^{18}\text{O}$ ,  $\text{C}^{16}\text{O}_2$ , and  $\text{C}^{18}\text{O}_2$ ) are shown in Fig. 2a as a function of reaction time. At the initial stage of the reaction, where CO conversion was less than 5%,  $\text{C}^{16}\text{O}_2$  had the highest mole fraction in  $\text{CO}_2$ , followed by  $\text{C}^{16}\text{O}^{18}\text{O}$  and  $\text{C}^{18}\text{O}_2$ . The mole fractions of  $\text{C}^{16}\text{O}^{18}\text{O}$  and  $\text{C}^{18}\text{O}_2$  increased, and that of  $\text{C}^{16}\text{O}_2$  decreased slowly at longer reaction times. However, no drastic change in the mole fraction was observed. Figure 2b shows the change in the atomic ratio of  $^{16}\text{O}$  in  $\text{CO}_2$  against reaction time. The initial atomic ratio of  $^{16}\text{O}/(^{16}\text{O} + ^{18}\text{O})$  in the total reactant molecules was 0.33. If the CO oxidation follows a reaction mechanism in which CO is oxidized with gas phase oxygen or with adsorbed oxygen without exchanging with lattice  $\text{O}^{2-}$ , the ratio of  $^{16}\text{O}$  in  $\text{CO}_2$  will remain constant at 0.50 throughout the reaction. On the contrary, if CO is oxidized only with lattice  $\text{O}^{2-}$ , the ratio of  $^{16}\text{O}$  in  $\text{CO}_2$  will be 1. As can be seen in Fig. 2b, from the initial stage of the reaction, the fraction of  $^{16}\text{O}$  in  $\text{CO}_2$  attained a level of 0.73 (after 3 min) and then decreased very slowly with reaction time. It is worthwhile to note that the isotopic exchange of oxygen between CO and gas phase  $^{18}\text{O}_2$  did not occur to any significant extent during this experiment. These results suggest that the lattice oxygen of ferrisilicate has been incorporated into the  $\text{CO}_2$  produced. Interestingly, the isotopic composition of any point in Fig. 2a is in statistical equilibrium; i.e., the ratio of  $(^{16}\text{O}^{18}\text{O})^2/(^{16}\text{O}_2)(^{18}\text{O}_2) = 4$ . This indicates that the oxygen atoms in

the  $\text{CO}_2$  equilibrate rapidly among themselves. In ferrisilicate, each  $\text{Fe}^{3+}$  ion occupies a tetrahedral coordination site surrounded by  $\text{SiO}_4^{4-}$  tetrahedra and is therefore connected to four oxygen (ions). After 20 h reaction time, the amount of lattice oxygen incorporated into the  $\text{CO}_2$  produced was equivalent to 1.8 times the amount of the oxygen connected to the framework iron of ferrisilicate. Therefore, it is suggested that the exchangeable lattice oxygen is not limited to the oxygen (ions) which are directly connected to  $\text{Fe}^{3+}$  but includes all the lattice oxygen. Mobility of lattice oxygen in aluminosilicate zeolites has been reported in the literature (28–30). Endoh *et al.* have studied the  $^{18}\text{O}$  exchange between  $\text{CO}_2$  and GaZSM-5 (30). In the case of GaZSM-5 prepared by dipping highly siliceous zeolite in sodium gallate solution, about six framework oxygen atoms per inserted Ga atom became reactive for the exchange.

In order to clarify whether the lattice oxygen which is not connected to  $\text{Fe}^{3+}$  in ferrisilicate can be incorporated into  $\text{CO}_2$ , CO oxidation was carried out with 5 mg of ferrisilicate at 773 K. After 20 h reaction time, CO conversion reached 71%, and the amount of lattice oxygen incorporated into  $\text{CO}_2$  was equivalent to four times the amount of oxygen connected to the framework  $\text{Fe}^{3+}$  of ferrisilicate; that is, about 16 framework oxygen atoms per framework  $\text{Fe}^{3+}$  were reactive for the exchange. The unit-cell formula of MFI-type ferrisilicate used here is  $\text{Na}_2\text{Fe}_2\text{Si}_{94}\text{O}_{192} \cdot 16\text{H}_2\text{O}$ . Therefore, the amount of oxygen incorporated into  $\text{CO}_2$  corresponds to 17% of the total lattice oxygen in ferrisilicate. It is concluded that not only the lattice oxygen adjacent to  $\text{Fe}^{3+}$  but also other lattice oxygen is available for incorporation into  $\text{CO}_2$  during the CO oxidation. Moreover, as was shown in Fig. 1a, the progress of the CO oxidation on ferrisilicate was extremely slow without gas phase oxygen. Therefore, it is clear that the incorporation of lattice oxygen cannot be achieved through the direct oxidation of CO by the lattice oxygen to form  $\text{CO}_2$ . There must be other routes by which the lattice oxygen becomes incorporated into  $\text{CO}_2$ . A rapid isotope exchange between the oxygen in  $\text{CO}_2$  and the lattice oxygen of the ferrisilicate could be the alternative route. Therefore it is necessary to verify this possibility experimentally.

#### Heterophase Exchange of Oxygen Isotope between $\text{C}^{18}\text{O}_2$ and Ferrisilicate

The reaction between  $\text{C}^{18}\text{O}_2$  and ferrisilicate was conducted under the following conditions:  $P(\text{C}^{18}\text{O}_2)$ , 5 Torr; amount of catalyst, 0.20 g; reaction temperature, 673 K. Results obtained in this experiment are shown in Fig. 3. The mole fractions of  $\text{CO}_2$  isotope were plotted against reaction time. The appearance of  $\text{C}^{16}\text{O}_2$  and  $\text{C}^{16}\text{O}^{18}\text{O}$  in the product implies an exchange between the lattice oxy-

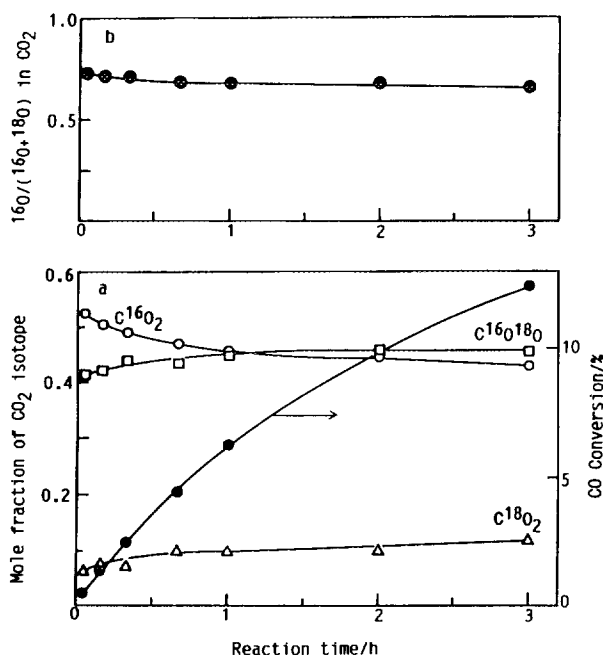


FIG. 2. CO oxidation with  $^{18}\text{O}_2$  at 673 K on ferrisilicate (25 mg). (a) Mole fractions of  $\text{C}^{16}\text{O}^{18}\text{O}$  ( $\square$ ),  $\text{C}^{16}\text{O}_2$  ( $\circ$ ), and  $\text{C}^{18}\text{O}_2$  ( $\triangle$ ) in  $\text{CO}_2$  and CO conversion ( $\bullet$ ), and (b) atomic ratio of  $^{16}\text{O}/(^{16}\text{O} + ^{18}\text{O})$  in  $\text{CO}_2$  were plotted against reaction time. Initial pressure of both CO and  $^{18}\text{O}_2$  was 30 Torr.

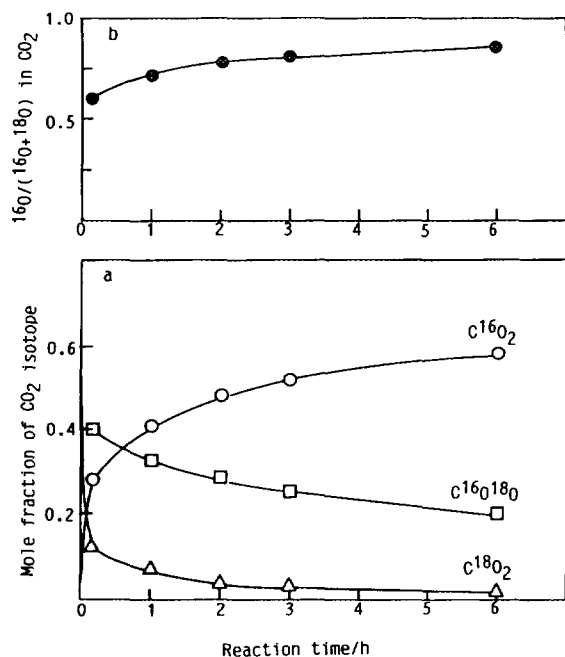


FIG. 3. Reaction of C<sup>18</sup>O<sub>2</sub> with lattice oxygen of ferrisilicate at 673 K using 0.02 g of ferrisilicate and 5 Torr of C<sup>18</sup>O<sub>2</sub>.

gen and CO<sub>2</sub>. At the initial stage of the reaction, the mole fractions of C<sup>16</sup>O<sub>2</sub> and C<sup>16</sup>O<sup>18</sup>O increased from zero, and that of C<sup>18</sup>O<sub>2</sub> decreased drastically from 1.0%. As shown in Fig. 3b, the atomic ratio of <sup>16</sup>O/(<sup>16</sup>O + <sup>18</sup>O) in CO<sub>2</sub> increased from zero (reactant) to 0.6 at the initial stage. These results indicate that the rate of heterophase exchange between C<sup>18</sup>O<sub>2</sub> and lattice oxygen (<sup>16</sup>O) is very fast. After the first few minutes, the mole fraction of C<sup>16</sup>O<sup>18</sup>O started to decrease, while that of C<sup>16</sup>O<sub>2</sub> kept increasing and that of C<sup>18</sup>O<sub>2</sub> declined further. After 6 h reaction time, 85% of the <sup>18</sup>O in the initial C<sup>18</sup>O<sub>2</sub> has been exchanged with the lattice oxygen of ferrisilicate which is equivalent to 2.2% of the total lattice oxygen. From the above results we conclude that in the CO oxidation on ferrisilicate the CO<sub>2</sub> produced undergoes a rapid heterophase exchange with the lattice oxygen. Consequently, a high <sup>16</sup>O content in CO<sub>2</sub> was observed, which was not anticipated in the reaction mechanism, in which the adsorbed species of reactants (CO and O<sub>2</sub>) react to form the product (CO<sub>2</sub>).

#### Equilibration of C<sup>16</sup>O<sub>2</sub>-C<sup>18</sup>O<sub>2</sub> on Ferrisilicate

The equilibration of CO<sub>2</sub> isotopes on ferrisilicate (0.20 g) was performed at 673 K by introducing a mixture of C<sup>16</sup>O<sub>2</sub> (10 Torr) and C<sup>18</sup>O<sub>2</sub> (10 Torr) onto the catalyst so that the atomic ratio of <sup>16</sup>O to <sup>18</sup>O in the feed was 1 : 1. If only a homophase equilibration of CO<sub>2</sub> isotopes occurs on the catalyst surface, the mole fractions of C<sup>16</sup>O<sup>18</sup>O, C<sup>18</sup>O<sub>2</sub>, and C<sup>16</sup>O<sub>2</sub> will be 0.50, 0.25, and 0.25, respectively

at equilibrium (100% exchange). Figure 4a shows the changes in the mole fractions of CO<sub>2</sub> isotopes against the reaction time. After 5 min, the mole fraction of C<sup>16</sup>O<sup>18</sup>O, C<sup>16</sup>O<sub>2</sub>, and C<sup>18</sup>O<sub>2</sub> reached 0.40, 0.45, and 0.15, respectively, which already exceeded the homophase equilibrium composition. Figure 4b shows the change in the atomic ratio of <sup>16</sup>O/(<sup>16</sup>O + <sup>18</sup>O) in CO<sub>2</sub>. The ratio rose from an initial value of 0.50 to 0.71 within 5 min of reaction time. These results indicate that on ferrisilicate at the initial stage of the reaction, scrambling of oxygen isotopes both in gas phase and between gas and solid phase may be occurring with extreme rapidity. Later, the mole fraction of C<sup>16</sup>O<sub>2</sub> increased and the mole fractions of both C<sup>16</sup>O<sup>18</sup>O and C<sup>18</sup>O<sub>2</sub> decreased slowly with reaction time. The atomic ratio of <sup>16</sup>O increased further as time elapsed. From the above results, the incorporation of <sup>16</sup>O from ferrisilicate lattice into CO<sub>2</sub> isotopes is again clearly evident. After 6 h reaction time, 62% of the initial <sup>18</sup>O in CO<sub>2</sub> isotope has been exchanged with the lattice oxygen of ferrisilicate. Therefore, we can conclude that the reaction of CO<sub>2</sub> isotopes on ferrisilicate may proceed very rapidly via both homophase equilibration and heterophase exchange.

#### Mechanistic Approach for CO Oxidation on Ferrisilicate

From the results of kinetic and isotopic tracer studies, we explain the CO oxidation mechanism on ferrisilicate

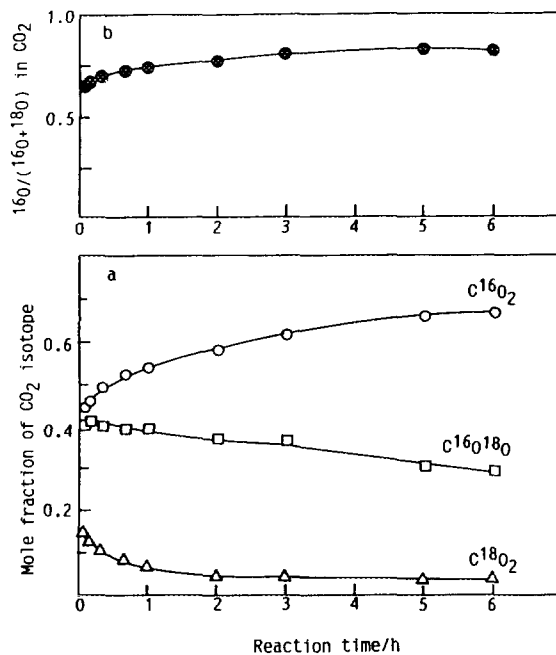


FIG. 4. C<sup>18</sup>O<sub>2</sub>-C<sup>16</sup>O<sub>2</sub> equilibration on ferrisilicate at 673 K. Weight of catalyst was 0.20 g and initial pressure of both C<sup>18</sup>O<sub>2</sub> and C<sup>16</sup>O<sub>2</sub> was 10 Torr.

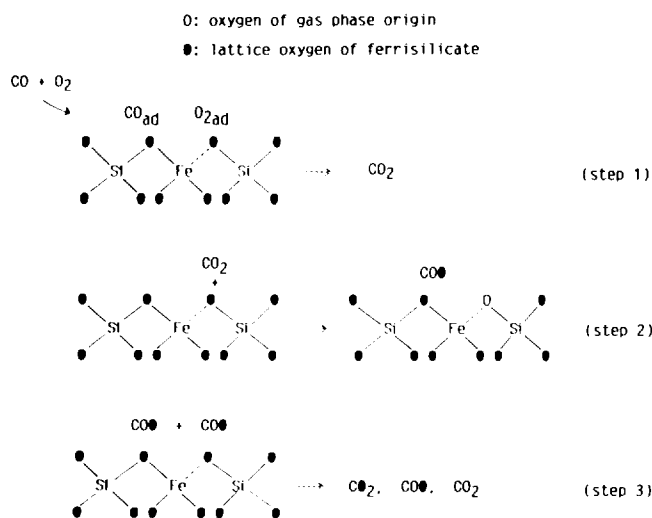


FIG. 5. Reaction scheme of CO oxidation with  $O_2$  on ferrisilicate.

with the help of the reaction scheme shown in Fig. 5. Adsorbed species of the reactants (CO and  $O_2$ ) on ferrisilicate react to form  $CO_2$  (step 1). The heterophase exchange between the lattice oxygen of ferrisilicate and  $CO_2$  produced occurs at a significant rate (step 2). Furthermore, the equilibration of oxygen isotopes in  $CO_2$  (step 3) occurs simultaneously on ferrisilicate. As a consequence, during the oxidation of CO, a significant amount of lattice oxygen in ferrisilicate is incorporated into  $CO_2$ .

#### CO Oxidation with $^{18}O_2$ on $FeO_x/Sil$

In order to clarify the mechanism of CO oxidation on  $FeO_x/Sil$  we performed the reaction of CO with  $^{18}O_2$  under the following conditions: amount of catalyst, 0.66 g;  $P(CO) = P(^{18}O_2)$ , 10 Torr; reaction temperature, 458 K (as the activity of  $FeO_x/Sil$  is much higher than that of ferrisilicate, the reaction was carried out at a lower temperature). In Fig. 6a, the mole fractions of  $CO_2$  isotopes are shown as a function of reaction time. In the initial stages of the reaction, the mole fraction of  $C^{16}O_2$  was comparatively high and then dropped drastically, while the mole fractions of  $C^{16}O^{18}O$  and  $C^{18}O_2$  increased with the lapse of time. Figure 6b shows the ratio of  $^{16}O/(^{16}O + ^{18}O)$  in  $CO_2$ . The ratio roughly approaches 1.0 when the reaction time is extrapolated to zero. The predominance of  $^{16}O$  in  $CO_2$  at the commencement of the reaction implies that lattice oxygen directly oxidized CO to form  $CO_2$  in the initial stages of the reaction. These results are consistent with the interpretation of the kinetics of CO oxidation on  $FeO_x/Sil$ . The catalyst amount used in this experiment corresponds to the amount of lattice oxygen required to oxidize the total amount of CO (10 Torr) introduced initially. As can be seen in Fig. 6b the ratio of  $^{16}O/(^{16}O + ^{18}O)$  in  $CO_2$  decreased significantly

with time in the initial stages of the reaction and then became virtually constant. This means that only a small portion of the original lattice oxygen of  $Fe_2O_3$  in  $FeO_x/Sil$  is involved in the CO oxidation. Moreover, it was shown in Fig. 1b that without gas phase oxygen the rate of CO oxidation was very slow compared with CO oxidation in the presence of gas phase oxygen. In order to get further insight into the reaction mechanism of CO oxidation on  $FeO_x/Sil$ , a series of experiments were carried out varying reaction conditions such as the amount of catalyst and the reaction temperature. Results of these experiments are shown in Fig. 7. In all cases, the mole fractions of  $CO_2$  isotopes changed slightly in the initial stages of the reaction; however, they became virtually constant in the later stages. After 1 h of reaction time, a similar result was obtained in all cases: the mole fractions of  $C^{16}O^{18}O$ ,  $C^{16}O_2$ , and  $C^{18}O_2$  were in the range 0.50–0.52, 0.26–0.27, and 0.22–0.24, respectively. These values are close to those of an equilibrium mixture of  $CO_2$  with  $^{16}O/^{18}O = 1$ , which could be obtained through the reaction of  $C^{16}O$  with  $^{18}O$  followed by equilibration. In such a case, the portion of the product formed by the reaction involving original lattice oxygen ( $^{16}O$ ) must be small. This can be explained in the following way: the reaction takes place upon the surface layer of  $Fe_2O_3$  crystallite supported on

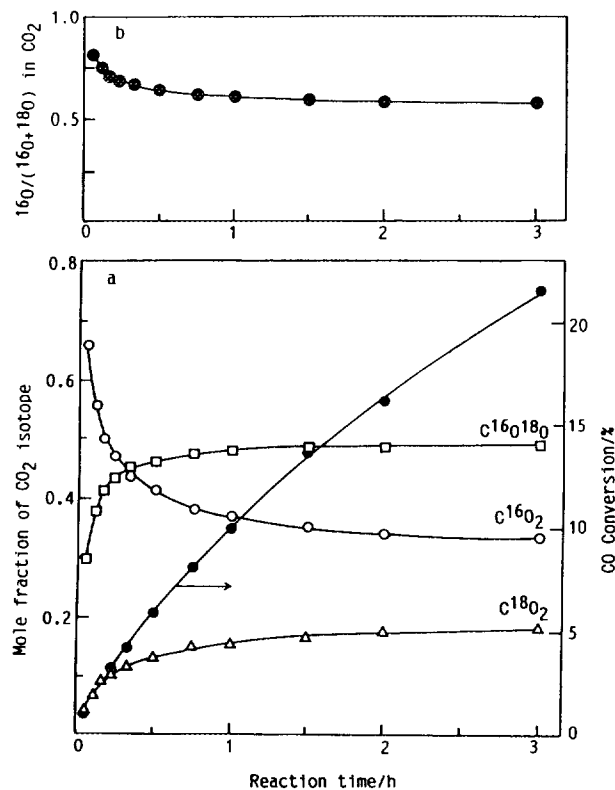


FIG. 6. CO oxidation with  $^{18}O_2$  on  $FeO_x/Sil$  at 458 K. Weight of catalyst was 0.66 g and initial pressure of both CO and  $^{18}O_2$  was 10 Torr.

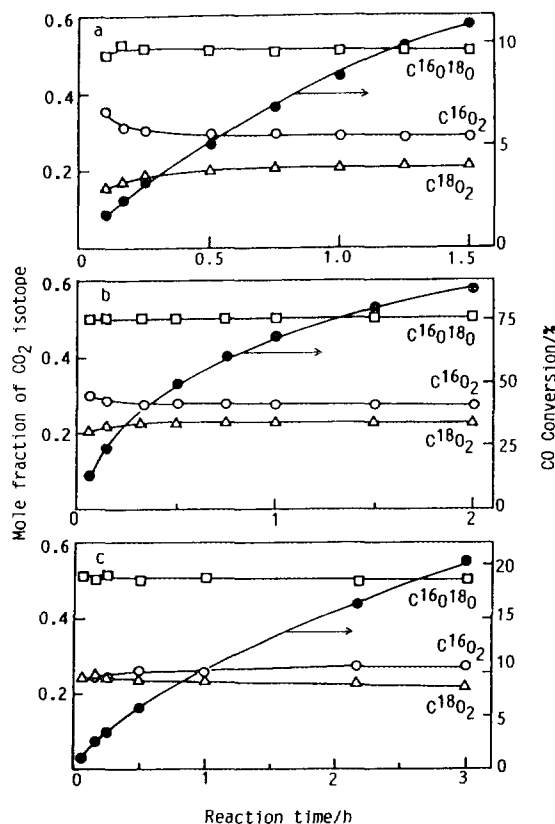


FIG. 7. CO oxidation with  $^{18}\text{O}_2$  on  $\text{FeO}_x/\text{Sil}$  at varying weight of catalyst and reaction temperature: (a) 0.13 g, 473 K; (b) 0.26 g, 523 K; (c) 0.33 g, 458 K. Initial pressure of both CO and  $^{18}\text{O}_2$  was 10 Torr.

silicalite, the oxygen vacancies where CO has been oxidized with the lattice oxygen are regenerated with  $^{18}\text{O}$  from the gas phase, and the scrambling of the lattice oxygen between the surface and the bulk of  $\text{Fe}_2\text{O}_3$  crystallite takes place very slowly compared with the CO oxidation. Accordingly, the composition of product containing  $^{16}\text{O}$ , at first high, falls during the course of the reaction (Fig. 6). In fact, after 16 h of the reaction under the condition in Fig. 6, only 3.3% of the lattice oxygen in  $\text{Fe}_2\text{O}_3$  had appeared in  $\text{CO}_2$ . The isotopic composition of any point in Figs. 6a and 7a–c is in statistical equilibrium, which means the oxygen atoms in the  $\text{CO}_2$  equilibrate rapidly among themselves.

#### Heterophase Exchange of Oxygen Isotope between $\text{C}^{18}\text{O}_2$ and $\text{FeO}_x/\text{Sil}$

The reaction between  $\text{C}^{18}\text{O}_2$  and  $\text{FeO}_x/\text{Sil}$  was conducted under the following conditions:  $P(\text{C}^{18}\text{O}_2)$ , 5 Torr; catalyst weight, 0.20 g; reaction temperature, 523 K. After 3 h reaction time, mole fractions of  $\text{C}^{16}\text{O}_2$ ,  $\text{C}^{16}\text{O}^{18}\text{O}$ , and  $\text{C}^{18}\text{O}_2$  reached 0.003, 0.077, and 0.920, respectively. From a material balance for oxygen isotopes, it was found that only 4.0% of the initial  $\text{C}^{18}\text{O}_2$  had been exchanged

with the lattice oxygen of  $\text{FeO}_x/\text{Sil}$  after 3 h reaction time, which is equivalent to 6.8% of the lattice oxygen in  $\text{Fe}_2\text{O}_3$  crystallites.

#### Equilibration of $\text{C}^{16}\text{O}_2$ – $\text{C}^{18}\text{O}_2$ on $\text{FeO}_x/\text{Sil}$

Figure 9 shows the results of the equilibration of  $\text{C}^{16}\text{O}_2$ – $\text{C}^{18}\text{O}_2$  on  $\text{FeO}_x/\text{Sil}$  performed at 523 K. The mole fraction of  $\text{CO}_2$  isotopes was plotted against the reaction time in Fig. 8a. At the beginning, the mole fractions of  $\text{C}^{16}\text{O}^{18}\text{O}$ ,  $\text{C}^{16}\text{O}_2$ , and  $\text{C}^{18}\text{O}_2$  were 0.46, 0.31, and 0.23, respectively, and remained virtually constant throughout the course of the reaction. It can be revealed that the rate of equilibration was too fast for measurement under the reaction conditions. Figure 8b shows the change in the atomic ratio of  $^{16}\text{O}/(^{16}\text{O} + ^{18}\text{O})$  in  $\text{CO}_2$  isotopes. The ratio remained almost constant in the range 0.53–0.54. In the case of ferrisilicate (Fig. 4b), the ratio of  $^{16}\text{O}$  in  $\text{CO}_2$  rose from an initial value of 0.50 to 0.71 within 5 min of reaction time, and increased further as time elapsed. Therefore, we conclude that the equilibration of  $\text{CO}_2$  isotopes occurs on  $\text{FeO}_x/\text{Sil}$  very rapidly; however, the extent of the incorporation of lattice oxygen into gas phase was very low compared with ferrisilicate.

#### Mechanistic Approach for CO Oxidation on $\text{FeO}_x/\text{Sil}$

In light of the above results, the reaction mechanism of CO oxidation on  $\text{FeO}_x/\text{Sil}$  could be explained. As shown in Fig. 9, CO oxidation on  $\text{FeO}_x/\text{Sil}$  proceeds via

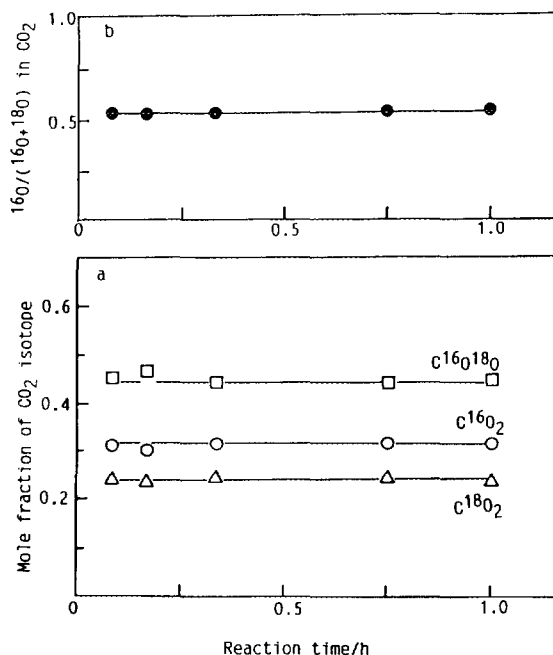


FIG. 8.  $\text{C}^{18}\text{O}_2$ – $\text{C}^{16}\text{O}_2$  equilibration on  $\text{FeO}_x/\text{Sil}$  at 523 K. Weight of catalyst was 0.20 g and initial pressure of both  $\text{C}^{18}\text{O}_2$  and  $\text{C}^{16}\text{O}_2$  was 10 Torr.

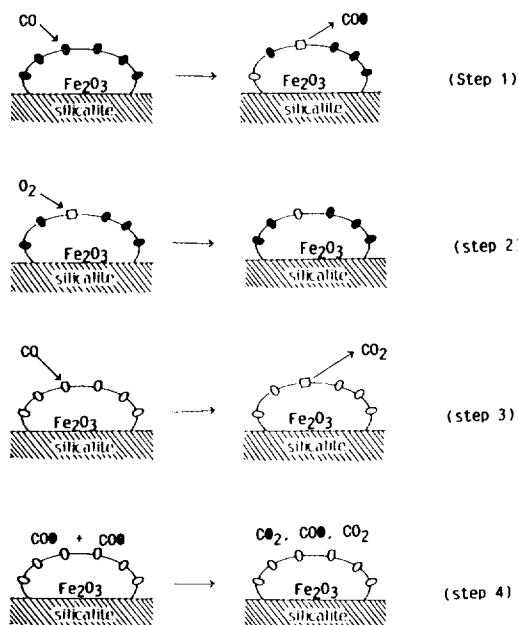


FIG. 9. Reaction scheme of CO oxidation with  $O_2$  on  $Fe_2O_3$ .

alternate reduction and oxidation of the iron-oxide ( $Fe_2O_3$ ) surface, and thus oxygen from the  $Fe_2O_3$  lattice appears in  $CO_2$  produced at the initial stage (step 1). The reaction takes place primarily upon the surface layer of  $Fe_2O_3$  crystallite, and the reduced site (oxygen vacancy) is rapidly reoxidized with gas phase oxygen (step 2). As the reaction proceeds, the surface lattice oxygen is largely replaced by gas phase oxygen. However, the scrambling of lattice oxygen between the surface and the bulk of  $Fe_2O_3$  occurs much more slowly than CO oxidation. Thus, at this stage, the  $CO_2$  produced contains only oxygen of gas phase origin (step 3). Therefore, the amount of lattice oxygen incorporated into  $CO_2$  is very small. The equilibration of oxygen isotopes in  $CO_2$  occurs very quickly (step 4). The mole fractions of  $CO_2$  isotopes remain almost constant in the later stages of the reaction.

#### REFERENCES

- Vedrine, J. C., in "Guidelines for Mastering the Properties of Molecular Sieves" (D. Barthomeuf *et al.*, Eds.), NATO ASI series, Vol. 221, p. 121. Plenum, New York, 1990.
- Namba, S., Iwase, O., Takahashi, N., Yashima, T., and Hara, N., *J. Catal.* **56**, 445 (1979).
- Barrer, R. M., "Hydrothermal Chemistry of Zeolites," p. 419. Academic Press, London, 1982.
- Szostak, R., Nair, V., and Thomas, T. T., *J. Chem. Soc., Faraday Trans.* **83**, 487 (1987).
- Inui, T., Matsuda, H., Yamase, O., Nagata, H., Fukuda, K., Ukawa, T., and Miyamoto, A., *J. Catal.* **98**, 491 (1986).
- Chu, C. T., and Chang, C. D., *J. Phys. Chem.* **89**, 1569 (1985).
- Borade, R. B., Halgeri, A. B., and Prasado Rao, T. S. R., in "New Development in Zeolite Science and Technology" (Y. Murakami *et al.*, Eds.), Studies in Surface Science and Catalysis, Vol. 28, p. 851. Elsevier-Kodansha, Amsterdam/Tokyo, 1986.
- Kim, J.-H., Namba, S., and Yashima, T., *Zeolites* **11**, 59 (1991).
- Lin, D. H., Coudrier, G., and Vedrine, J. C., in "Zeolites: Facts, Figures, Future" (P. A. Jacobs and R. A. Van Santen, Eds.), Studies in Surface Science and Catalysis, Vol. 49B, p. 1431. Elsevier, Amsterdam, 1989.
- Notari, B., in "Innovation in Zeolite Materials Science" (P. A. Jacobs and J. A. Martens, Eds.), Studies in Surface Science and Catalysis, Vol. 37, p. 413. Elsevier, Amsterdam, 1987.
- Miyamoto, A., Medhanavyn, D., and Inui, T., in "Proceedings, 9th International Congress on Catalysis, Calgary, 1988" (M. J. Phillips and M. Ternan, Eds.), Vol. 1, p. 437. Chem. Institute of Canada, Ottawa, 1988.
- Lowenstein, W., *Amer. Mineral.* **39**, 92 (1954).
- Petunchi, J. O., and Hall, W. K., *J. Catal.* **80**, 403 (1983).
- Kubo, T., Tominaga, H., and Kurugi, T., *Bull. Chem. Soc. Jpn.*, **46**, 3549 (1973).
- Aparicio, L. M., Ulla, M. A., Millman, W. S., and Dumesic, J. *Catal.* **110**, 330 (1988).
- Matsumoto, H., and Tanabe, S., *J. Phys. Chem.* **14**, 420 (1990).
- Benn, F. R., Dwyer, J., Esfahani, A., Evmerides, N. P., and Szczepura, A. K., *J. Catal.* **48**, 60 (1977).
- Bobrov, N. N., Borestov, G. K., Ione, K. G., Terletsikh, A., and Shestakova, N. A., *Kint. Katal.*, **15**, 413 (1974).
- Ione, K. G., Bobrov, N. N., Borestov, G. K., and Vostrova, L. A., *Dokl. Akad. Nauk. SSR* **210**, 388 (1973).
- Petunchi, J. O., and Hall, W. K., *J. Catal.* **78**, 327 (1982).
- Jin, T., Okuhara, T., Mains, G. J., and White, J. M., *J. Phys. Chem.* **91**, 3310 (1987).
- Meagher, A., Nair, V., and Szostak, R., *Zeolites* **8**, 3 (1988).
- Uddin, Md. A., Komatsu, T., and Yashima, T., *Microporous Materials* **1**, 201 (1993).
- Galuszka, J., Sano, T., and Sawicki, J. A., *J. Catal.* **136**, 96 (1992).
- Kouenhowen, H. W., and Stork, W. H., U.S. Patent 4,208,305 (1980).
- Ball, W. J., Dwyer, J., Garforth, A. A., and Smith, W. J., in "New Development in Zeolite Science and Technology" (Y. Murakami *et al.*, Eds.), Studies in Surface Science and Catalysis, Vol. 28, p. 137. Elsevier-Kodansha, Amsterdam/Tokyo, 1986.
- Flanigen, E. M., Bennett, J. R., Grose, R. W., Cohen, J. P., Patton, R. L., Kirchner, R. M., and Smith, J. V., *Nature* **271**, 512 (1978).
- Fripiat, J. J., in "Catalysis by Zeolites" (B. Imelik *et al.*, Eds.), Studies in Surface Science and Catalysis, Vol. 5, p. 161. Elsevier, Amsterdam, 1980.
- Yamagishi, K., Namba, S., and Yashima, T., *J. Phys. Chem.* **95**, 872 (1991).
- Endoh, A., Nishimiya, K., Tsutsumi, K., and Takahashi, T., in "Zeolites as Catalyst, Sorbent and Detergent Builders" (H. G. Karge and J. Weitkamp, Eds.), Studies in Surface Science and Catalysis, Vol. 46, p. 779, Elsevier, Amsterdam, 1989.